

Advances in Brief

Automated Quantification of Apoptosis after Neoadjuvant Chemotherapy for Breast Cancer: Early Assessment Predicts Clinical Response¹

Darren W. Davis, Thomas A. Buchholz,
Kenneth R. Hess, Aysegül A. Sahin,
Vincente Valero, and David J. McConkey²

Departments of Cancer Biology [D. W. D., D. J. M.], Radiation Oncology [T. A. B.], Biostatistics [K. R. H.], Pathology [A. A. S.], and Breast Medical Oncology [V. V.], The University of Texas M.D. Anderson Cancer Center, Houston, Texas 77030

Abstract

Purpose: A large body of evidence implicates apoptosis in the effects of cancer chemotherapeutic agents on tumor cells *in vitro* and tumor xenografts *in vivo*, but the predictive value of apoptosis as an early marker for clinical response in cancer patients remains unclear.

Experimental Design: We developed an automated, laser scanning cytometer-based method to quantify the percentage of tumor cells containing DNA fragmentation characteristic of apoptosis in tumor sections. We measured levels of apoptosis in a panel of 15 matched, 18-gauge core breast cancer biopsies obtained before and 48 h after neoadjuvant therapy with docetaxel plus doxorubicin or paclitaxel as part of two prospective clinical trials.

Results: The results revealed a strongly significant ($P = 0.0023$) association between chemotherapy-induced apoptosis and pathological response.

Conclusions: If the results can be validated in a larger patient cohort, the method could be used to “tailor” therapy to optimize benefit in a patient-specific fashion.

Introduction

Apoptosis is a form of physiological cell death characterized at the biochemical level by the activation of a family of cysteine proteases known as caspases, which results in DNA fragmentation (1). Work conducted over the past decade has

demonstrated that the molecular control of apoptosis is evolutionarily conserved and that it participates in a diverse array of physiological and pathological responses (1, 2). In particular, many studies have demonstrated that cancer therapies can induce apoptosis in tumor cells (3, 4), but almost all of this evidence is derived from experiments with cells in culture or with experimental models of human cancer. Although it appears likely that apoptosis also contributes to the activity of many conventional cancer chemotherapeutic agents in human patients, this has not been established, presumably because highly sensitive, quantitative methods for detecting apoptosis in tissue sections have not been available. The potential value of an assay that would allow for early prediction of drug efficacy is self evident, particularly for the patients with tumors refractory to particular chemotherapeutics.

We recently adapted a conventional method for detecting apoptosis-associated DNA fragmentation (the TUNEL³ technique) to allow for automated quantification of cell death using a LSC (5). The LSC (Compucyte, Inc., Cambridge, MA) is an instrument designed to quantify the intensity of up to five independent fluorescent probes simultaneously at the single cell level in a fashion that is essentially analogous to fluorescence-activated cell sorting. Advantages of LSC-based quantification over standard manual methods include its higher sensitivity and analytical power: tens of thousands of cells can be routinely analyzed in each tissue section, as opposed to the hundreds of cells typically evaluated in standard 3–5 high power field manual approaches. Because determination of positive and negative is accomplished objectively (by gating against staining controls), the method should also be more reproducible in the hands of different investigators. Here we used the LSC to quantify the percentages of TUNEL-positive cells in 18-gauge core biopsies obtained from patients on two institutional Institutional Review Board-approved prospective clinical trials of neoadjuvant cytotoxic therapy [doxorubicin (Adriamycin) plus docetaxel (Taxotere; the “AT” regimen)] or paclitaxel alone.

Patients and Methods

Patient Selection and Treatment. Thirty patients with breast cancer scheduled to begin definitive treatment with neoadjuvant chemotherapy were enrolled in the study. A core biopsy was requested at study entry, and again at 24 and 48 h after treatment. Each patient consented to undergo serial core biopsies, but the post-treatment biopsies were not mandatory. All of the patients were informed about the investigational

Received 7/29/02; revised 11/14/02; accepted 11/14/02.

The costs of publication of this article were defrayed in part by the payment of page charges. This article must therefore be hereby marked *advertisement* in accordance with 18 U.S.C. Section 1734 solely to indicate this fact.

¹ Supported by grants from Physicians Referral Service, University of Texas M. D. Anderson Cancer Center (to T. A. B.) and National Cancer Institute (U54 CA090810, to D. J. M.). All of the LSC analyses were conducted within a confocal microscopy and image analysis core facility (Dr. Michael Andreeff, Director) that is supported by the Cancer Center Support Grant CA16672 awarded by the National Cancer Institute, Department of Health and Human Services.

² To whom requests for reprints should be addressed, at Department of Cancer Biology, 173, University of Texas M.D. Anderson Cancer Center, 1515 Holcombe Boulevard, Houston, TX 77030. Phone: (713) 792-8591; Fax: (713) 792-8747; E-mail: dmconcke@mdanderson.org.

³ The abbreviations used are: TUNEL, terminal deoxynucleotidyl transferase-mediated nick end labeling; LSC, laser scanning cytometer; wk, weekly; CR, complete response; PR, partial response; AT, doxorubicin/docetaxel; FAC, 5-fluorouracil/doxorubicin/cyclophosphamide.

Table 1 Chemotherapy, tumor characteristics, levels of apoptosis, and clinical responses
Patients were treated with the indicated primary regimens before surgery.

Patient	1st chemo	Cycles	Dose	2nd chemo	Cycles	ER ^a	PR	Her2	Path. response	Clin. response	Apoptosis baseline	Apoptosis 24 h	Apoptosis 48 h
1	wk taxol	12	175	FAC	4	pos	neg	neg	CR	PR	0.80%	0.98%	9.12%
2	AT	4	60/60	none		pos	pos	na	CR	CR	3.88%	4.18%	36.89%
3	AT	4	60/60	none		neg	pos	pos	CR	near CR	0.33%	nd	9.61%
4	AT	4	60/60	none		neg	neg	neg	<1 cm	PR	2.09%	1.60%	6.84%
5	AT	4	60/60	none		neg	pos	unk	<1 cm	PR	0.81%	nd	11.89%
6	AT	4	60/60	none		neg	neg	neg	<1 cm	PR	0.02%	1.31%	3.46%
7	AT	6	60/60	none		pos	neg	pos	<1 cm	PR	0.06%	11.91%	nd
8	AT	4	60/60	none		pos	neg	na	<1 cm	PR	4.59%	2.09%	12.18%
9	AT	6	60/60	CMF	3	neg	neg	neg	3 cm	PR	0.99%	1.20%	nd
10	taxol q3	4	175	FAC	4	pos	pos	pos	2 cm	near CR	0.29%	0.24%	0.21%
11	AT	6	60/60	none		pos	pos	neg	5.3 cm	PR	0.30%	6.13%	3.52%
12	AT	4	60/60	none		neg	pos	neg	4 cm	PR	0.14%	1.03%	0.01%
13	wk taxol	12	60/60	FAC	4	neg	neg	neg	1.4 cm	PR	1.22%	10.68%	0.88%
14	AT	4	60/60	none		neg	neg	pos	progressed	progressed	0.60%	0.06%	0.50%
15	wk taxol	12	80	FAC	4	pos	pos	neg	progressed	progressed	0.72%	nd	0.84%

^a ER, estrogen receptor; PR, progesterone receptor; CMF, cyclophosphamide/methotrexate/5-fluorouracil; q3, 3-weekly.

nature of the study and gave informed consent according to institutional and federal guidelines.

Patients enrolled in the study received treatment as part of two prospective clinical trials. The first involved bolus neoadjuvant AT given every 3 weeks ($n = 20$). One patient on this regimen received a secondary regimen of cyclophosphamide/methotrexate/5-fluorouracil before surgery. The second involved single-agent paclitaxel (Taxol), given in a randomized study comparing a 3-wk ($n = 5$) versus a wk schedule ($n = 5$) followed by a secondary regimen of 5-fluorouracil (500 mg/m²), doxorubicin (50 mg/m²), and cyclophosphamide (500 mg/m²; FAC) before surgery (Table 1).

Tumor Biopsies. The goal of this study was to perform one baseline and two post-treatment biopsies (24 and 48 h) on every participant. Biopsies were obtained under local anesthetic using a spring-loaded 18-gauge core needle (Bard Co, Inc., GA). Post-treatment cores were performed using the same skin entry site as the baseline biopsy. Approximately 4–6 cores were obtained during each biopsy session. The biopsies were formalin-fixed and embedded in paraffin. All of the core biopsies were stained with H&E and reviewed by a pathologist to confirm the presence of tumor tissue.

Of the 30 participants, 24 had a baseline biopsy, and 8 of these elected not to undergo the post-treatment biopsies. One patient developed a bone metastasis and did not undergo any subsequent biopsies. Fifteen patients had a post-treatment biopsy at 24 h, and 1 patient elected not to undergo a 48 h biopsy. Three biopsies at 24 h and 1 at 48 h had too little or no tumor available for analysis. Thus, the levels of apoptosis reported in this study are derived from 15 biopsies obtained before therapy, 12 biopsies obtained 24 h after treatment, and 13 biopsies obtained 48 h after treatment (see Table 1).

TUNEL. Thin (4- μ m) sections were prepared, mounted on slides, and DNA fragmentation was analyzed by TUNEL (6) using a commercial kit (Promega, Inc., Madison, WI). Tissue sections were deparaffinized in xylene, rehydrated in alcohol, and transferred to PBS. Tissues were then fixed in 4% paraformaldehyde at room temperature for 10 min and washed twice for

5 min with PBS. Next, tissues were incubated with 20 μ g/ml proteinase K for 10 min at room temperature. After two 5-min washes with PBS, tissues were preincubated with terminal deoxynucleotidyl transferase buffer for 10 min at room temperature. Avoiding light, the reaction buffer was added to the tissue sections, and the slides were incubated in a humid atmosphere at 37°C for 1 h. The tissues were washed twice (5 min each) with PBS and stained with 1 μ g/ml propidium iodide for 10 min. Slides were washed again three times for 5 min. Cover slips were mounted using Prolong (Molecular Probes, Eugene, OR). Immunofluorescence microscopy was performed using a $\times 200$ objective (Zeiss Plan-Neofluar) on an epifluorescence microscope equipped with narrow bandpass excitation filters mounted in a filter wheel to select for green and red fluorescence. Images were captured using a chilled CCD camera (Hamamatsu) on a PC computer and were processed using Adobe Photoshop software (Adobe Systems, Mountain View, CA).

LSC Analysis. The LSC (CompuCyte Corporation) is an instrument designed to enable fluorescence-based quantitative measurements on tissue sections or other cellular preparations at the single-cell level. The instrument consists of a base unit containing an Olympus BX50 fluorescent microscope, and an optics/electronics unit coupled to an argon and HeNe laser that repeatedly scans along a line as the surface is moved past it on a computer-controlled motorized stage. Before LSC analysis, biopsies were evaluated by fluorescence microscopy to ensure optimal fluorescent staining. The LSC was used to determine the percentage of tumor cells undergoing apoptosis in each core biopsy. For analysis, each slide was placed on a computer-controlled motorized stage. The desired area to be scanned was visually located using the microscope of the instrument, and the tumor region was mapped using the Wincyte software. Slides were scanned using a $\times 200$ objective, and cell nuclei were contoured using the argon laser and red detector (propidium iodide). TUNEL-positive events were detected using the argon laser and green detector. Similar to flow cytometry (fluorescence-activated cell sorting), the relative levels of fluorescence intensity were recorded on a scatterplot defined by four quadrants. A

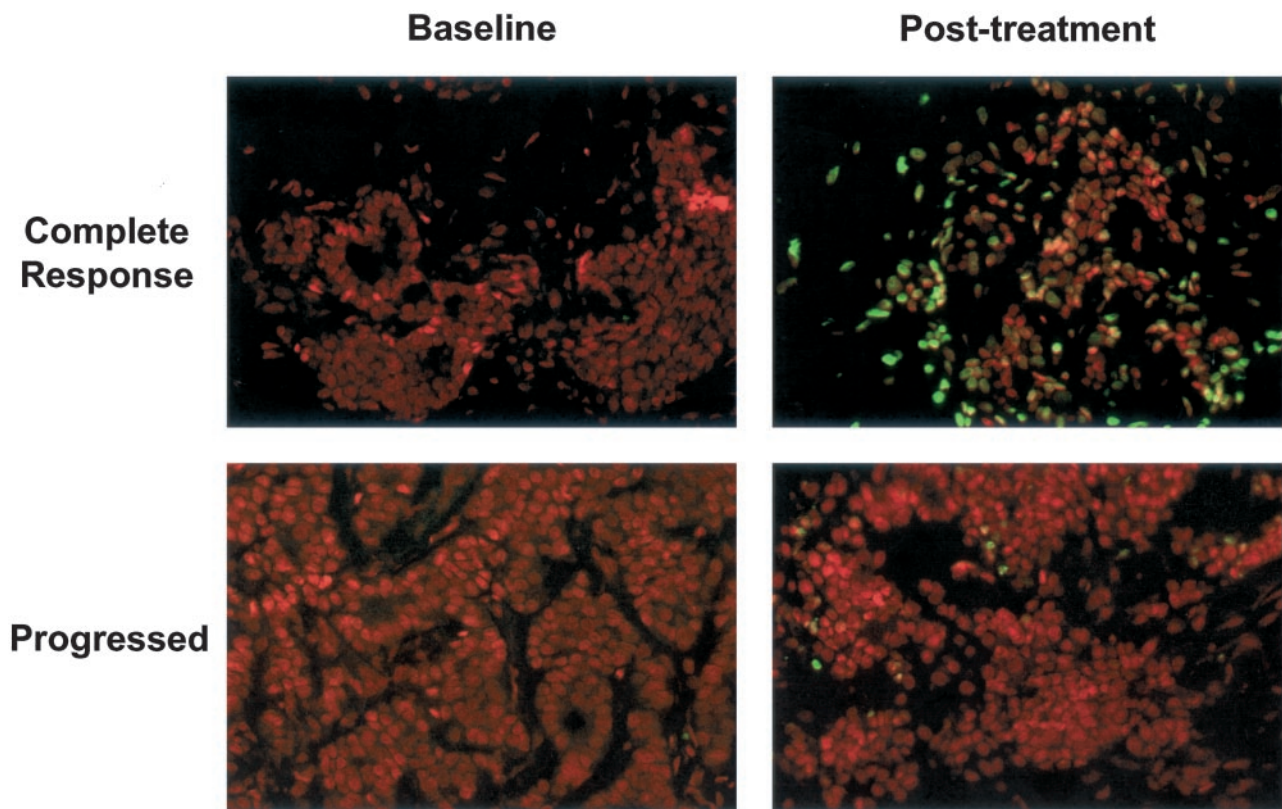


Fig. 1 Qualitative analysis of DNA fragmentation. Apoptosis-associated DNA fragmentation was detected by fluorescent TUNEL (green), and total cell nuclei were detected by counterstaining with propidium iodide (red). Representative fluorescence microscopic ($\times 200$ objective) images obtained from baseline and after treatment (48 h) tumors are presented for 1 of the patients who demonstrated a pathological CR and 1 of the patients who progressed on therapy.

negative control slide was used to determine the analytical gates for each sample. Relocation was used to visually confirm TUNEL-positive cells. Once the gates were set, the data file was played to determine the percentage of TUNEL-positive cells in each core biopsy.

Immunohistochemistry. The avidin-biotin complex method was used for immunohistochemical staining and applied to paraffin-embedded tissue sections of pre- and post-treatment samples. Serial sections were cut at 4- μm , deparaffinized with xylene, and rehydrated through a series of graded ethanol. The immunohistochemical procedure was performed using an automated stainer (DAKO, Carpinteria, CA). The primary antibodies were used against estrogen receptor ID5 (Zymed Laboratories), progesterone receptor 1A6 (Novacastra Laboratories), and Her-2/*neu* AB8 (NeoMarkers). The antigen-antibody immunoreaction was visualized using 3-3'-diaminobenzidine as the chromogen, and the slides were counterstained with light hematoxylin. The nuclear staining of $>5\%$ of tumor nuclei was considered to be positive for estrogen and progesterone receptors. Her-2/*neu* expression was scored as the percentage of cells with complete and strong membranous staining, and specimens were considered Her2-/*neu*-positive when $>10\%$ of cells exhibited staining.

Statistical Methods. The primary end point used to determine the correlation between apoptosis and the primary che-

motherapeutic regimen was the pathological response of the primary tumor, evaluated by the extent of residual disease present after the surgical procedure. Pathological response was divided into four categories: (a) CR, absence of invasive breast cancer at the primary; (b) PR with residual breast disease <1 cm; (c) response with residual breast disease >1 cm; and (d) clinical evidence of progressive disease during chemotherapy (progressed; see Table 1). For statistical analysis, we grouped pathological response into two categories: "excellent" = 1, 2, and "poor" = 3, 4. We compared the distribution of 24-h and 48-h changes in tumor cell apoptosis from baseline between these two response categories. Because the data values contained outliers, we used the Wilcoxon rank sum test to compare the two independent samples represented by the response categories. Because the sample sizes are relatively small, we used the exact, permutation version of this test.

Results

Biopsies were collected just before initiation of the first cycle of systemic therapy, 24 h after chemotherapy, and again at 48 h after chemotherapy. These biopsies were obtained with signed patient-informed consent. Pathological responses were evaluated at the time of surgery. The 15 tumors analyzed in this study were diverse in terms of clinical prognostic markers and in

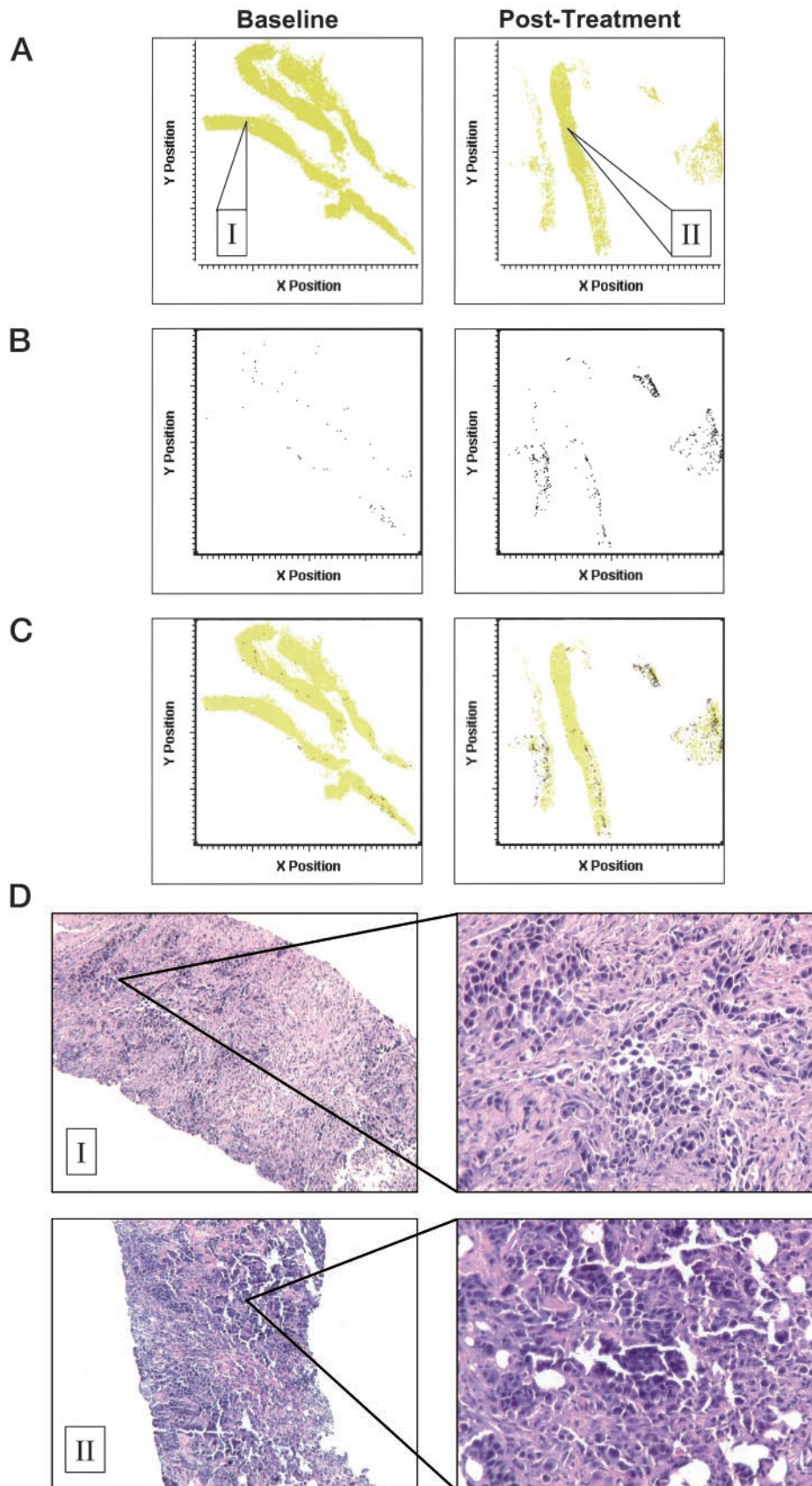


Fig. 2 Identification and localization of TUNEL-positive cells by LSC. *A*, representative contour map of total cell nuclei. Tumor sections were stained using fluorescent TUNEL and propidium iodide as described in "Materials and Methods." The slides were analyzed by LSC, and all of the cell nuclei identified by propidium iodide were plotted on an *x* and *y* coordinate map. Representative contour maps corresponding to biopsies obtained before and 48 h after therapy are presented. *B*, contour map of apoptosis. The same slides analyzed in *A* were subsequently interrogated for TUNEL fluorescence, and the apoptotic cells were plotted on an *x* and *y* coordinate map. Note the increase in density of apoptotic cells after therapy. *C*, overlay of *A* and *B*. The cell nuclei and apoptosis contour maps were superimposed to demonstrate the localization of the TUNEL-positive cells with respect to total tumor cellularity. Note that apoptotic tumor cells are scattered throughout the biopsy. *D*, analysis of tumor morphology by H&E staining. The sections analyzed in *A*–*C* above were subsequently stained with H&E. Contour maps were generated and used to identify tumor regions corresponding to the map generated in *A*. Regions corresponding to areas defined by *I* and *II* in *A* are presented (original magnification: $\times 40$ and $\times 200$).

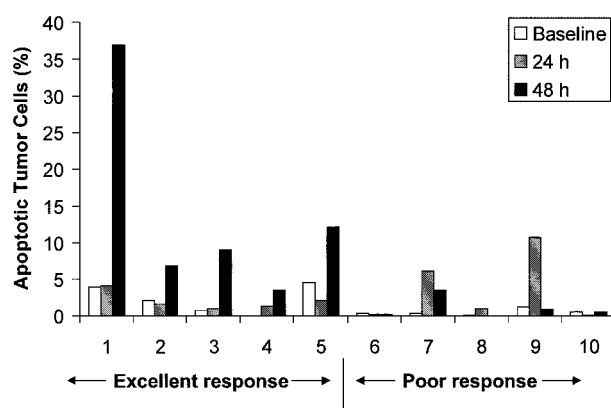


Fig. 3 A, quantification of apoptosis by LSC. TUNEL-positive cells were quantified in whole tumor core biopsy sections and expressed as a percentage of total cells (determined by propidium iodide staining). Raw cell death percentages are presented for patients with both a 24-h and 48-h post-treatment biopsy. Note that the patients are arranged according to the nature of their clinical response (excellent response is defined as residual tumor <1 cm, and poor response is defined as residual tumor >1 cm as described in "Patients and Methods"). Only patients that were biopsied at 24 h and 48 h were included in the figure ($n = 10$). Note that all patients with an excellent response demonstrated higher levels of tumor cell apoptosis at 48 h after treatment compared with baseline.

their responses to neoadjuvant therapy, as described in detail in Table 1. Slides were stained using the TUNEL technique and counterstained with propidium iodide to visualize cell nuclei. Representative TUNEL images obtained before and after therapy in a tumor that underwent a complete pathological response and a tumor that progressed on therapy are presented in Fig. 1. Qualitative analysis revealed that the levels of apoptosis increased in biopsies obtained from tumors that underwent major pathological responses but were uniformly low in tumors that did not. Whole 4- μ m sections were then analyzed using an LSC as described in "Patients and Methods." Fig. 2 presents contour maps generated from one of the matched biopsy pairs obtained from a tumor that displayed an excellent response. Fig. 2A displays the locations of all of the tumor cells as determined by propidium iodide (red) staining before and 48 h after therapy. Fig. 2B indicates the positions of the apoptotic cells, identified by TUNEL (green) fluorescence, and Fig. 2C is overlays of the two images. Note that the number of TUNEL-positive cells increases in the biopsy obtained after therapy. The contour map obtained was then used to compare the fluorescence results with tumor morphology as detected by H&E staining. Fig. 2D displays the H&E-stained tumor regions corresponding to regions I and II in Fig. 2A.

LSC-mediated quantification was used to determine the percentage of tumor cell apoptosis in biopsies obtained at baseline, 24 h, and 48 h after neoadjuvant therapy (Fig. 3; Table 1). Patients were categorized by excellent response (those with no tumor at the primary or minimal residual disease <1 cm) or poor response (those with residual disease >1 cm or progressive disease). Note that all of the patients in the excellent response category demonstrated higher levels of tumor cell apoptosis at 48 h after treatment compared with baseline. Levels of tumor cell apoptosis at 24 h were consistently the same as baseline or

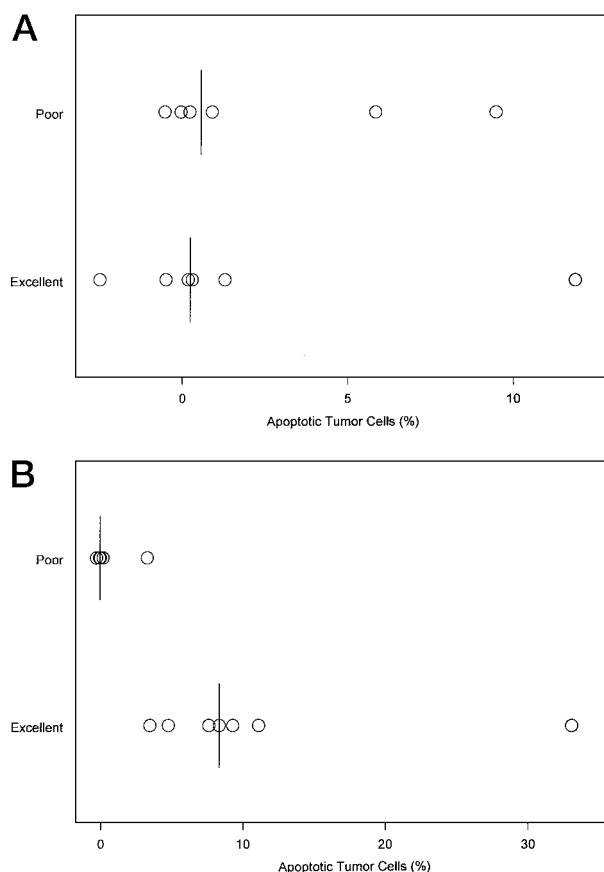


Fig. 4 Changes in apoptosis (48 h) correlate with response. Tumors were grouped into two categories, those that demonstrated excellent responses and those that demonstrated a poor response as described in "Patients and Methods." Data points corresponding to the percentage of change in individual tumor cell apoptosis at A, 24 h, and B, 48 h, are indicated by the open symbols. Group medians (excellent = 0.24% and 8.32%, poor = 0.55% and -0.09% for 24 h and 48 h, respectively) are indicated by the vertical lines. By these criteria rates of apoptosis correlated directly with response for 48 h ($P = 0.0023$) but not 24 h ($P = 0.82$) using the Wilcoxon rank sum test.

lower compared with 48 h after treatment with the exception of 2 cases in the poor response category. Indeed, changes in tumor cell apoptosis at 24 h after therapy were uniformly lower and did not correlate with pathological response of the tumors (Fig. 4A). In contrast, patients whose tumors displayed an excellent pathological response were significantly ($P = 0.0023$, Wilcoxon rank sum test) correlated to changes in tumor cell apoptosis at 48 h after therapy compared with tumors that displayed a poor pathological response (Fig. 4B).

Discussion

Laboratory investigation performed over the last decade has clearly established a role for apoptosis in chemotherapy-induced cell death (reviewed in Ref. 2). However, kinetic studies in solid tumor cell lines exposed to drugs *in vitro* demonstrate that a significant "lag" period is observed before detection of the first signs of DNA fragmentation (7). In our own previous studies gemcitabine-induced DNA fragmentation in orthotopic

tumor xenografts was not readily apparent at 24 h but was obvious by 48 h (8). These kinetics are quite consistent with those reported here, where in 9 of 10 cases the levels of apoptosis observed at 24 h were substantially lower than the levels observed at 48 h (Fig. 3). This fact likely explains why the 24-h data did not correlate with response. It is possible that quantitative evaluation of another biomarker of apoptosis (cytochrome *c* release, caspase-3 activation, and p53 activation) could provide predictive information before the appearance of significant DNA fragmentation, which is detected by the TUNEL technique. We are investigating this possibility at present.

Although analysis of our whole cohort of tumors demonstrated a significant correlation between apoptosis and clinical response, the value of an assay like this one likely will depend on its ability to predict response on a case-by-case basis. We would also hope that the magnitude of the increase in chemotherapy-induced apoptosis should correlate with the magnitude of the clinical response. It was not possible to distinguish the tumors that ultimately displayed a complete pathological response from those that displayed some residual tumor at the time of surgery or stable disease from progression. Furthermore, we did observe a few outliers in the data set, most importantly 1 tumor that displayed significant levels of apoptosis at 24 h but not at 48 h. Because apoptotic cells are rapidly cleared by tissue macrophages *in vivo* (9), any "snapshot" of apoptosis taken at a single time point will underestimate total levels of cell death. Furthermore, tumors are markedly heterogeneous, and it is therefore likely that the accuracy of results obtained by this and other biopsy-dependent techniques will be related to the extent to which the whole tumor is sampled. Together, these biological properties probably explain why we were not able to use our assay to predict the absolute magnitude of the clinical responses observed.

With rare exceptions, it is currently impossible to determine whether or not cancer therapy is effective before radiographic changes are evident, which typically takes weeks to occur. Physical examinations are relatively imprecise, and lack sensitivity and specificity. Furthermore, improvements in physical examination findings tend to occur near the second cycle of therapy, well into the treatment course. What this means for the patient is that effective therapeutic intervention is often significantly delayed or never obtained, resulting in unnecessary, prolonged exposure to agents that possess significant toxicity. The data reported in this study are consistent with results obtained by others using different methods suggesting that levels of therapy-induced apoptosis correlate with response (10–13). If

the results of this study can be confirmed in a larger patient cohort, using automated LSC analysis to monitor rates of apoptosis after therapy could provide clinical investigators with a more rational means of maximizing therapeutic benefit. As suggested above, it should also be possible to use the LSC to measure even earlier molecular changes (*i.e.*, receptor phosphorylation, cell cycle modulation) associated with effective drug-target interactions in patients treated with both conventional and biological agents.

References

- Hengartner, M. O. The biochemistry of apoptosis. *Nature (Lond.)*, 407: 770–776, 2000.
- Thompson, C. B. Apoptosis in the pathogenesis and treatment of disease. *Science (Wash. DC)*, 267: 1456–1462, 1995.
- Eastman, A. Activation of programmed cell death by anticancer agents: cisplatin as a model system. *Cancer Cells (Cold Spring Harbor)*, 2: 275–280, 1990.
- Johnstone, R. W., Ruefli, A. A., and Lowe, S. W. Apoptosis: a link between cancer genetics and chemotherapy. *Cell*, 108: 153–164, 2002.
- Davis, D. W., Weidner, D. A., Holian, A., and McConkey, D. J. Nitric oxide-dependent activation of p53 suppresses bleomycin-induced apoptosis in the lung. *J. Exp. Med.*, 192: 857–869, 2000.
- Gavrieli, Y., Sherman, Y., and Ben-Sasson, S. A. Identification of programmed cell death *in situ* via specific labeling of nuclear DNA fragmentation. *J. Cell Biol.*, 119: 493–501, 1992.
- McCloskey, D. E., Kaufmann, S. H., Prestigiacomo, L. J., and Davidson, N. E. Paclitaxel induces programmed cell death in MDA-MB-468 human breast cancer cells. *Clin. Cancer Res.*, 2: 847–854, 1996.
- Nawrocki, S. T., Bruns, C. J., Harbison, M. T., Bold, R. J., Gotsch, B. S., Abbruzzese, J. L., Elliott, P., Adams, J., and McConkey, D. J. Effects of the proteasome inhibitor PS-341 on apoptosis and angiogenesis in orthotopic human pancreatic tumor xenografts. *Mol. Cancer Ther.*, 1: 1243–1253, 2002.
- Savill, J., and Fadok, V. Corpse clearance defines the meaning of cell death. *Nature (Lond.)*, 407: 784–788, 2000.
- Chang, J., Ormerod, M., Powles, T. J., Allred, D. C., Ashley, S. E., and Dowsett, M. Apoptosis and proliferation as predictors of chemotherapy response in patients with breast carcinoma. *Cancer (Phila.)*, 89: 2145–2152, 2000.
- Symmans, W. F., Volm, M. D., Shapiro, R. L., Perkins, A. B., Kim, A. Y., Demaria, S., Yee, H. T., McMullen, H., Oratz, R., Klein, P., Formenti, S. C., and Muggia, F. Paclitaxel-induced apoptosis and mitotic arrest assessed by serial fine-needle aspiration: implications for early prediction of breast cancer response to neoadjuvant treatment. *Clin. Cancer Res.*, 6: 4610–4617, 2000.
- Symmans, F. W. Breast cancer response to paclitaxel *in vivo*. *Drug Resist Updat.*, 4: 297–302, 2001.
- Green, A. M., and Steinmetz, N. D. Monitoring apoptosis in real time. *Cancer J.*, 8: 82–92, 2002.

Clinical Cancer Research

Automated Quantification of Apoptosis after Neoadjuvant Chemotherapy for Breast Cancer: Early Assessment Predicts Clinical Response

Darren W. Davis, Thomas A. Buchholz, Kenneth R. Hess, et al.

Clin Cancer Res 2003;9:955-960.

Updated version Access the most recent version of this article at:
<http://clincancerres.aacrjournals.org/content/9/3/955>

Cited articles This article cites 13 articles, 6 of which you can access for free at:
<http://clincancerres.aacrjournals.org/content/9/3/955.full#ref-list-1>

Citing articles This article has been cited by 13 HighWire-hosted articles. Access the articles at:
<http://clincancerres.aacrjournals.org/content/9/3/955.full#related-urls>

E-mail alerts [Sign up to receive free email-alerts](#) related to this article or journal.

Reprints and Subscriptions To order reprints of this article or to subscribe to the journal, contact the AACR Publications Department at pubs@aacr.org.

Permissions To request permission to re-use all or part of this article, use this link
<http://clincancerres.aacrjournals.org/content/9/3/955>.
Click on "Request Permissions" which will take you to the Copyright Clearance Center's (CCC) Rightslink site.